Local properties of three-body atomic wave functions

R. Krivec,[1,*] V. B. Mandelzweig,[2,†] and K. Varga[3,‡]
[1]*Department of Theoretical Physics, J. Stefan Institute, P.O. Box 3000, 1001 Ljubljana, Slovenia*
[2]*Racah Institute of Physics, Hebrew University, Jerusalem 91904, Israel*
[3]*Physics Division, Argonne National Laboratory, 9700 South Cass Avenue, Argonne, Illinois 60439*
(Received 30 November 1999; published 9 May 2000)

The local properties and accuracy of the positronium negative-ion (Ps^-) ground-state wave functions obtained by the stochastic variational method (SVM) and by direct solution of the Schrödinger equation with the help of the correlation-function hyperspherical-harmonic method (CFHHM) are studied and compared. Though the energy, calculated by both methods, agrees to up to ten digits, the amplitudes of the values of the operator $D=H\Psi/E\Psi-1$, characterizing local deviation of the wave function from its true value, in all of the coordinate space in the SVM are consistently larger (by up to five orders of magnitude) than in the CFHHM, despite the fact that the SVM observables except $\langle\delta(\mathbf{r}_k)\rangle$ converge to significantly more digits than the CFHHM observables for their respective selected bases.

PACS number(s): 31.15.Ja, 31.15.Pf, 36.10.Dr

I. INTRODUCTION

The question of accurate calculation of wave functions of few-body Coulomb systems and the importance of knowledge of their proper analytical structure for the calculation of observables is of long standing. It was first raised in the literature by Bartlett *et al.* [1,2] many years ago and more recently discussed once again in Refs. [3,4]. Until recently, by far the most accurate estimates of observables were obtained in different variational calculations [5–9], which, however, sophisticated and precise as they currently are, are not able to reproduce the correct analytical structure of three-body wave functions, since the inclusion or omission of logarithmic terms [6], or negative powers of interparticle distances [3], has negligible effect on the value of the variational energy. A variational function coincides with the precise one only on the average, and can wildly or even infinitely deviate from it locally [3]. These local discrepancies could lead to wrong estimates of expectation values of different operators which have significant contributions from the regions of the configuration space where the deviations occur.

To allow a more quantitative discussion of this problem, we have compared the observables and the local properties of the positronium negative-ion (Ps^-) ground-state wave functions calculated by two contemporary methods, the stochastic variational method (SVM) [7,8], and the correlation-function hyperspherical-harmonic method (CFHHM) [10,11]. The local convergence and accuracy of wave functions obtained by the CFHHM were previously analyzed for ground and excited states of the helium atom and for the Ps^- ground state in Ref. [4], but the present comparison is especially interesting. On one side, the CFHHM is the only method that not only yields precision comparable to that obtained by elaborate variational calculations but by its nature of producing a direct solution of the few-body Schrödinger equation generates the correct analytic structure of the wave function, including proper logarithmic terms and imposing exactly the Kato cusp conditions. On the other side, the SVM yields extremely accurate expectation values, converged to many significant digits.

We restrict ourselves here to comparison of the wave functions obtained by these two methods though investigation of the wave functions produced by other precise methods could be very instructive as well. For example, the finite-element method, similarly to the CFHHM, yields accurate direct solution of the three-body Schrödinger equation [12]. Though it cannot, by virture of being a pure numerical method, show explicitly the analytic structure of the solution, the proper analysis of accuracy of its wave functions and their comparison with variational wave functions is certainly very interesting and should be done in the future.

Of the local properties of the CFHHM and SVM wave functions, Ψ_{CFHHM} and Ψ_{SVM}, the stress is on the relative local deviation $D=H\Psi/E\Psi-1$ and the derivatives at the coalescence points, which show directly to what extent the Kato cusp conditions are satisfied. These two quantities are extremely sensitive measures of the local goodness of the wave function and could be used therefore for proper judging of the accuracy of any method of solving the Schrödinger equation. For example, for a true eigenfunction D is strictly equal to zero. However, it becomes infinite at any of the singularities if they are not properly included in the calculated wave function, even when the wave function itself displays very smooth behavior [1,2,4].

In this paper the particles $\{1,2,3\}$ correspond to $\{e,e,p\}$, where e denotes an electron and p denotes the positron. The Jacobi vectors, the first connecting the kth pair and the second connecting the center of mass of the kth pair with the third particle, are denoted respectively by $\mathbf{r}_k$ and $\mathbf{s}_k$ (see Fig.

*Electronic address: rajmund.krivec@ijs.si
†Electronic address: victor@helium.fiz.huji.ac.il.
‡On leave from the Institute for Nuclear Research of the Hungarian Academy of Sciences (ATOMKI), P.O. Box 51, 4001 Debrecen, P.O. Box 51, Hungary. Electronic address: varga@theory.phy.anl.gov

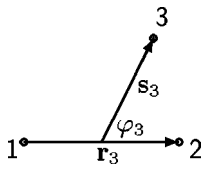

FIG. 1. Jacobi coordinates for a three-body system, for the pair index $k=3$.

1). The angle between $\mathbf{r}_k$ and $\mathbf{s}_k$ is denoted by φ_k. The odd-man-out notation for relative coordinates is used where single indices appear on quantities; frequently, the particle pairs are denoted explicitly for readability. Thus, $\mathbf{r}_1=\mathbf{r}_{ep}$. All results are given in atomic units.

In the SVM [7,8], the wave function is expanded in basis functions which usually, as well as in the present work, are of Gaussian type. The cusp conditions are not imposed on the wave function.

In the CFHHM [10,11], the wave function is decomposed as $\Psi_{\mathrm{CFHHM}}=e^f\Phi$, where f is the correlation function and Φ is a smooth function expandable in hyperspherical harmonics. The maximum global angular momentum used is denoted by K_{m} and corresponds to $N=(K_{\mathrm{m}}/4+1)^2$ basis functions.

The nonlinear parametrizations of f are of the form [11,13]

$$f=\sum_{k=1}^{3}\left[a_k+(b_k-a_k)e^{-r_k/(n_k\bar{r}_k)}\right]r_k, \tag{1}$$

where $\bar{r}_k$ are equilibrium interparticle distances, n_k are small numbers, and b_k are the cusp parameters. All f parametrizations satisfy the Kato cusp conditions exactly; a_k and n_k are free parameters, some of which are fixed by asymptotic conditions.

We use the fastest converging nonlinear f parametrization, denoted by ''B,'' used in Ref. [13]:

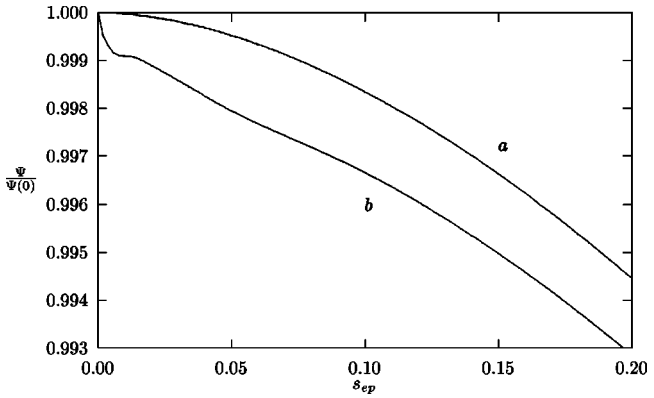

FIG. 2. CFHHM and SVM wave functions, normalized to 1 at the origin, for $r_{ep}=0$ and the favorable case $\varphi_{ep}=90°$, as functions of s_{ep}. Curve *a*: CFHHM, $K_{\mathrm{m}}=100$, parametrization B; Curve *b*: SVM, $N=800$. s_{ep} is in a.u.

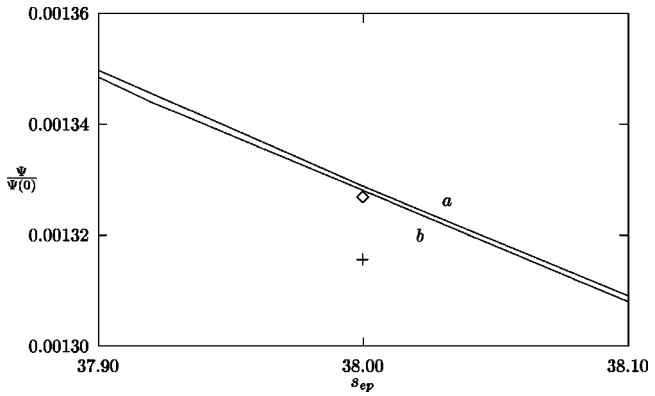

FIG. 3. As in Fig. 2 (curves *a* and *b*), but at large distances. ◇: CFHHM, $K_{\mathrm{m}}=80$; +: CFHHM, $K_{\mathrm{m}}=56$.

$$f=-0.5r_1e^{-r_1/(n_1\bar{r}_1)}-0.5r_2e^{-r_2/(n_2\bar{r}_2)}-(-0.126\,517\,825+0.626\,517\,825e^{-r_3/(n_3\bar{r}_3)})r_3, \tag{2}$$

in which a_3 was fixed from asymptotic conditions, and the remaining optimized values are $a_1=a_2=0$, $n_1=n_2=n_3=5$. (For this work the previous Ps^- calculation [13] was extended to $K_{\mathrm{m}}=100$.)

II. OBSERVABLES

The CFHHM expectation values with the parametrization B should be calculated with K_{m} at least 100 to give nine-digit precision in energy. At this K_{m} the oscillatory convergence of observables also becomes negligible.

Table I contains the final CFHHM and SVM as well as classical exponential variational expansion (EVE) [9] estimates of different Ps^- expectation values and their errors. We note that in the CFHHM K_{m} could be increased still further, but for the purpose of the present discussion the precision reached is sufficient. Comparing expectation values in Table I and taking coincident digits in observables obtained by the two different methods as the true ones we make the following conclusions.

(i) The CFHHM with $K_{\mathrm{m}}=100$, which includes 676 hyperspherical basis functions, yields energy convergent to nine significant digits (SD), $\langle\delta(\mathbf{r}_{ep})\rangle$ to eight SD; $\langle\delta(\mathbf{r}_{ee})\rangle$ to 6–7 SD, and negative and positive powers of interparticle distances to six and five SD, respectively.

(ii) The SVM with 800 basis functions produces energy convergent to twelve SD; $\langle\delta(\mathbf{r}_{ep})\rangle$ to four SD; $\langle\delta(\mathbf{r}_{ee})\rangle$ to three SD, and negative and positive values of powers of interparticle distances to twelve and ten SD, respectively.

III. DIRECT COMPARISON OF Ψ

Figure 2 shows the different behavior of the CFHHM and SVM wave functions, arbitrarily normalized to 1 at the origin, at the attractive coalescence point ($r_{ep}=0$), as functions of s_{ep}. It appears that the Gaussian-type basis used in the SVM calculation causes undulations of the order of 0.002 in the detailed behavior of Ψ_{SVM} near the origin due to insufficient convergence. Ψ_{CFHHM} for $K_{\mathrm{m}}=56$, 80, and 100 can-

TABLE I. CFHHM, SVM, and EVE observables. $N=676$ (CFHHM), $N=800$ (SVM), and $N=1000$ (EVE). The CFHHM values are presented with error estimates in parentheses. Square brackets denote the powers of 10. For values other than $\langle H\rangle$, the converged digits are given, but not more than 12 (rounded).

Operator	CFHHM	SVM [7,8]	EVE [9]
$\langle H\rangle$	0.262 005 069 5	0.262 005 070 226	0.262 005 070 232 965
$\langle r_{ep}\rangle$	5.489 6(1)	5.489 633 252 180	5.489 633 252 37
$\langle r_{ee}\rangle$	8.548 5(2)	8.548 580 655 061	8.548 580 655 12
$\langle r_{ep}^{-1}\rangle$	0.339 822(1)	0.339 821 023 027	0.339 821 023 059
$\langle r_{ee}^{-1}\rangle$	0.155 633(1)	0.155 631 905 632	0.155 631 905 653
$\langle r_{ep}^{-2}\rangle$	0.279 327 2(1)	0.279 326 539 097	0.279 326 542 159
$\langle r_{ee}^{-2}\rangle$	0.036 022 3(2)	0.036 022 059 431	0.036 022 058 49
$\langle \delta(\mathbf{r}_{ep})\rangle$	0.020 733 14(6) [a]	0.020 731 048 976	0.020 733 198 0
$\langle \delta(\mathbf{r}_{ee})\rangle$	0.170 997(2)[−3]	0.171 112 600 741[−3]	0.170 996 99[−3]

[a]The globally corrected value of $\langle \delta(\mathbf{r}_{ee})\rangle$, [14] 0.020 733 17(3), newly calculated in the present work, has an error twice as small.

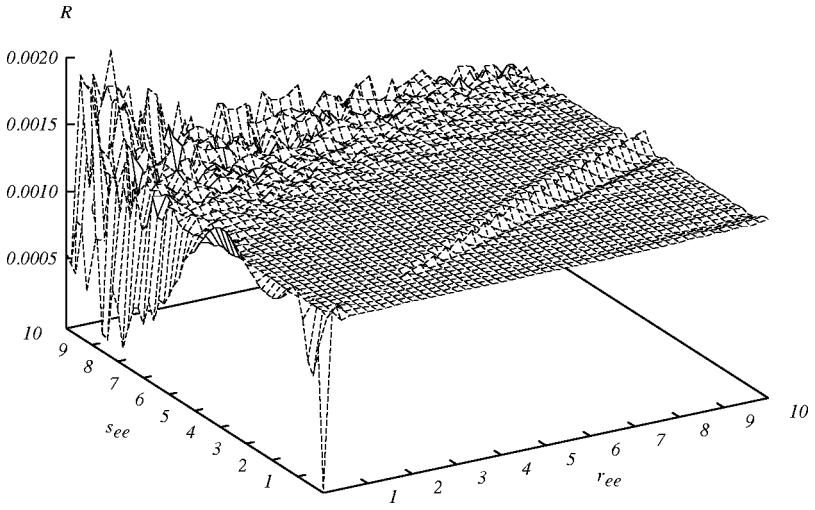

FIG. 4. Relative difference of the CFHHM and SVM wave functions, $R=(\Psi_{\mathrm{CFHHM}}-\Psi_{\mathrm{SVM}})/\Psi_{\mathrm{SVM}}$, for $r_{ee},s_{ee}\leq 10$ a.u., $\varphi_{ee}=1°$. CFHHM: $K_{\mathrm{m}}=80$; SVM: $N=800$. The wave functions are normalized to 1 at the origin. r_{ee} and s_{ee} are in a.u.

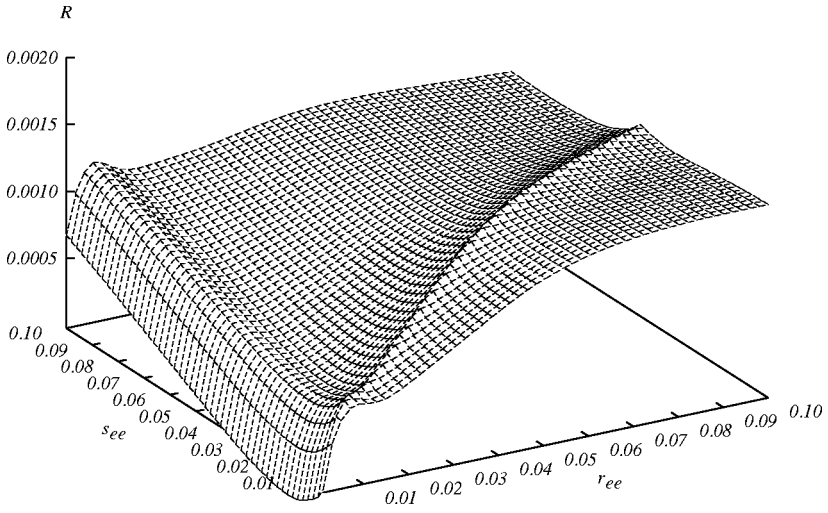

FIG. 5. As in Fig. 4, but for $r_{ee},s_{ee}\leq 0.1$ a.u.

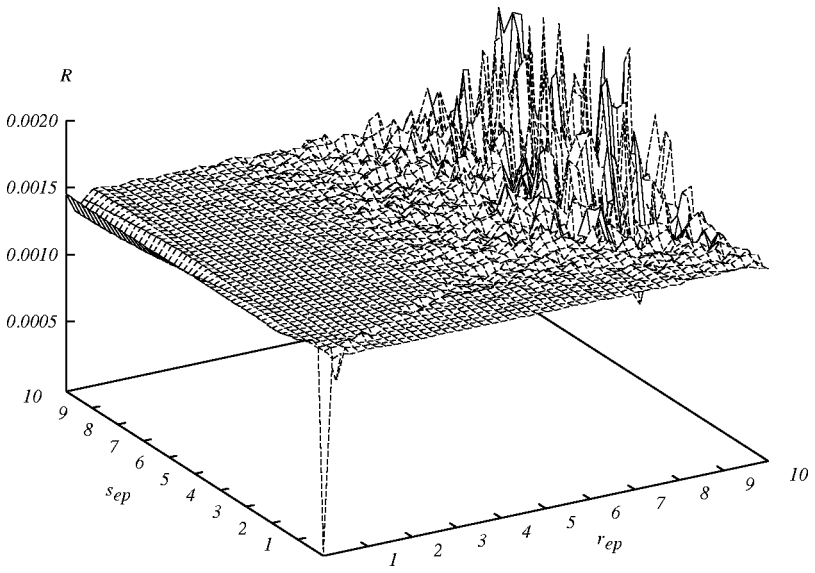

FIG. 6. As in Fig. 4, but in the r_{ep}, s_{ep} coordinates; $r_{ep}, s_{ep} \leqslant 10$ a.u., $\varphi_{ep} = 1°$.

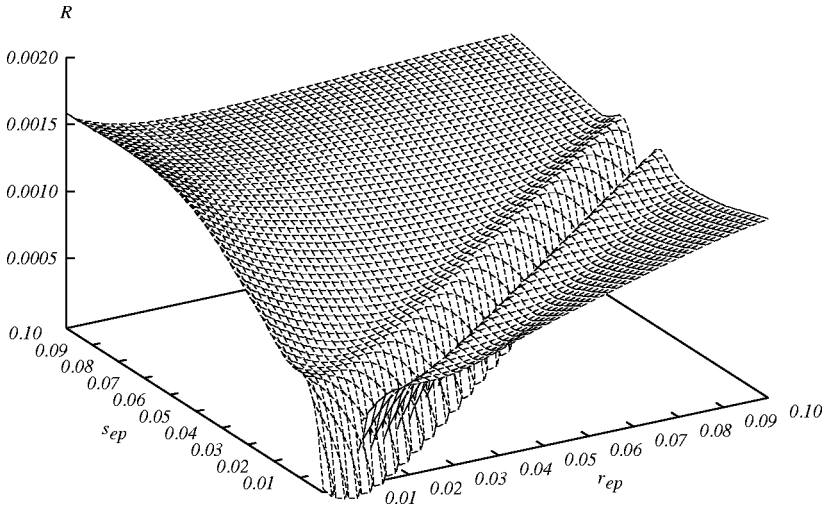

FIG. 7. As in Fig. 6, but for $r_{ep}, s_{ep} \leqslant 0.1$ a.u.

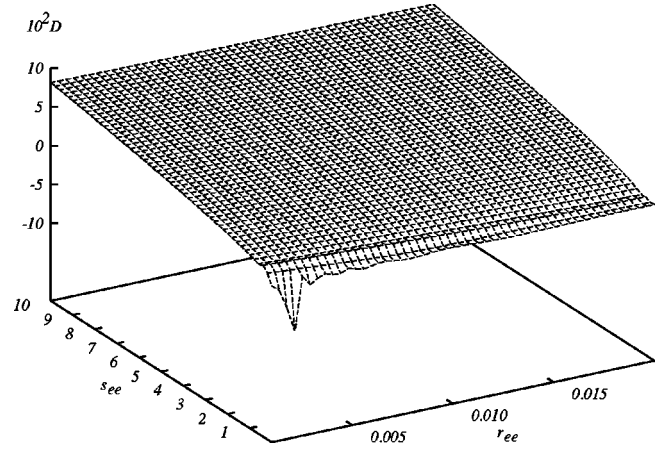

FIG. 8. $D = H\Psi/E\Psi - 1$ in percent (i.e., $10^2 D$) for the CFHHM, $K_{\mathrm{m}} = 100$, in a narrow rectangular region adjoining the s_{ee} axis, where 0 a.u. $< r_{ee} < 0.02$ a.u., 0 a.u. $< s_{ee} < 10$ a.u.

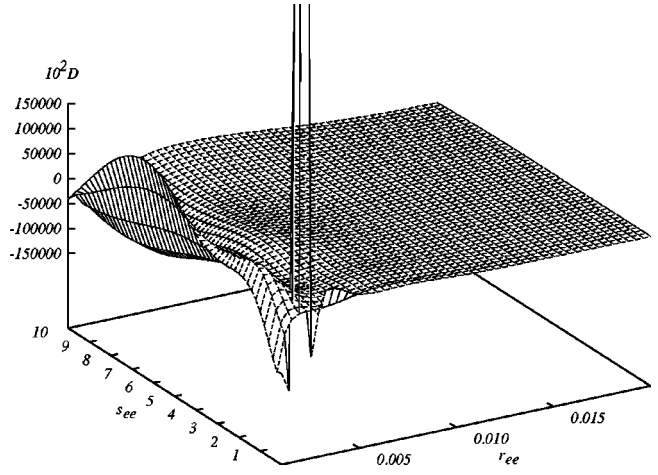

FIG. 9. As in Fig. 8, but the SVM, $N = 800$. The D surface in the SVM has a more short-range structure and much larger amplitudes of the D values than in the CFHHM: the D scale is 15 000 times larger than in Fig. 8.

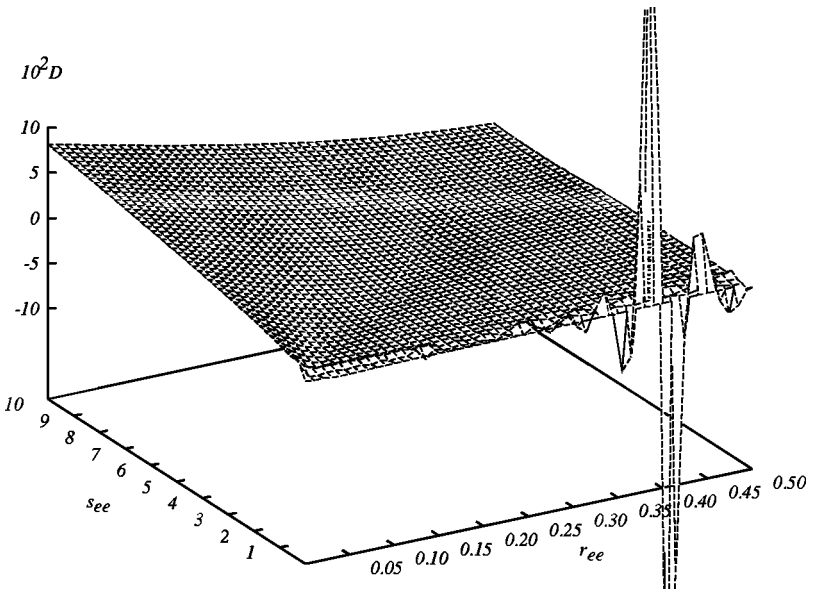

FIG. 10. As in Fig. 8, but the CFHHM D surface in a wider region along the s_{ee} axis (0 a.u. $<r_{ee}<0.5$ a.u., 0 a.u. $<s_{ee}<10$ a.u.), to show more structure due to the its more extended nature.

not be distinguished in Fig. 2. Figure 3 shows the same wave functions at large distances, and at smaller vertical scale. The extent of CFHHM convergence is shown by comparison of the points obtained with $K_{\mathrm{m}}=56$ and $K_{\mathrm{m}}=80$ at $\mathbf{s}_{ep}=38$ a.u. Ψ_{CFHHM} and Ψ_{SVM} agree to within the error of Ψ_{CFHHM} convergence, i.e., to a few times 10^{-6}.

Figures 4–7 show the relative differences of Ψ_{CFHHM} and Ψ_{SVM}, $R=(\Psi_{\mathrm{CFHHM}}-\Psi_{\mathrm{SVM}})/\Psi_{\mathrm{SVM}}$, in the parts of configuration space relevant for expectation value calculation. Wave functions are normalized to 1 at the origin, so that the rather different behavior at the origin enforces a relative difference of the order of 1×10^{-3} in the regions up to about the equilibrium distances. However, only the variations of R across the coordinate space are relevant; small differences in the normalizations of Ψ_{SVM} or Ψ_{CFHHM} would only shift the R axis, but not change the surfaces. The oscillating deviations at large distances are partly due to finite grid size. The undulations at small distances are presumably caused by the SVM wave function.

IV. RELATIVE LOCAL DEVIATION OF Ψ

In this section we show figures of the relative local deviation $D=H\Psi/E\Psi-1$ for the unfavorable case when φ_k is 1°, where the particles are almost at the coalescence point if their distances are appropriate. (If φ_k is 90°, the surfaces are almost flat.) Here E is the value of energy corresponding to the ground-state wave function. This value in both methods coincides to up to the tenth significant figure and is displayed in the first line of Table I.

Figures 8, 9, and 10 show the values of relative local deviation D in percent for the CFHHM and SVM, in narrow regions of coordinate space near the s_{ee} axis, i.e., where r_{ee} is small. The D surfaces have structure which appears at different scales for the CFHHM and SVM; to present more detail, we give two different r_{ee} scales for the CFHHM. The amplitudes of the SVM values are about five orders of magnitude larger than the amplitudes of the CFHHM values.

The sharp peaks in Figs. 9 and 10 are spurious: they cor-

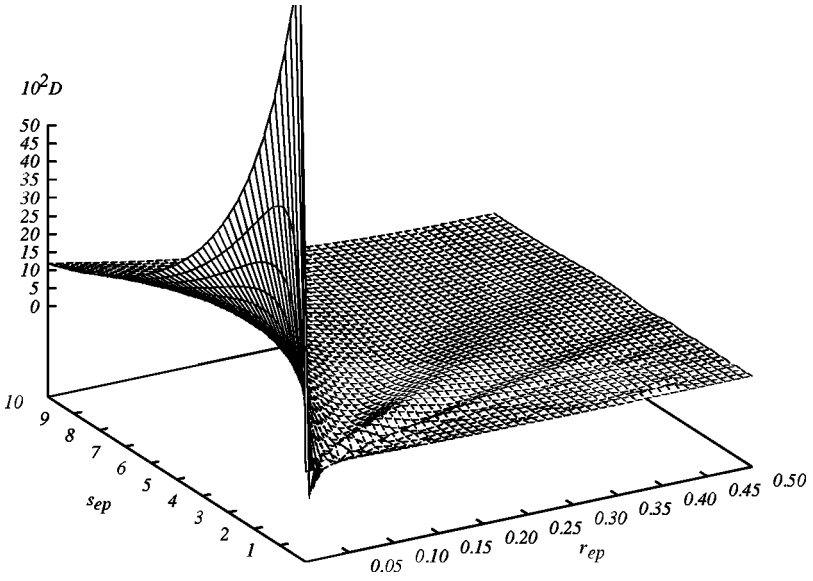

FIG. 11. As in Fig. 10, but the CFHHM D surface in coordinates r_{ep}, s_{ep} (0 a.u. $<r_{ep}<0.5$ a.u., 0 a.u. $<s_{ep}<10$ a.u.).

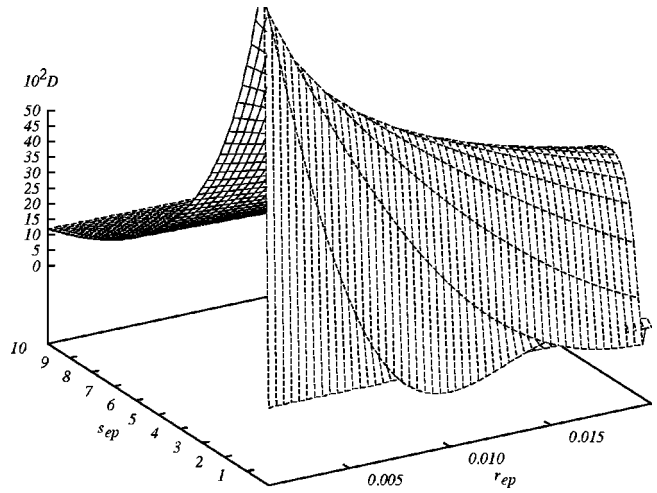

FIG. 12. As in Fig. 11, but in a narrow region adjoining the s_{ep} axis (0 a.u. $<r_{ep}<0.02$ a.u., 0 a.u. $<s_{ep}<10$ a.u.).

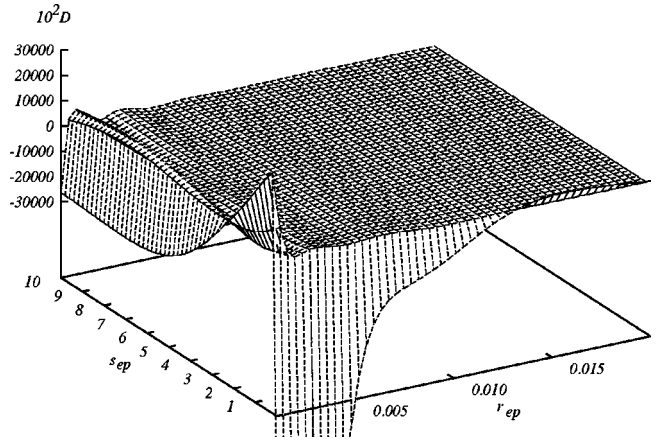

FIG. 13. As in Fig. 12, but the SVM, $N=800$. The D surface in the SVM has a more short-range structure than in the CFHHM and larger amplitudes of the D values. The D scale is 1200 times larger than in Fig. 12.

respond to points near the attractive coalescence point ($r_{ep}=0$), which because of the finite density of the plotting grid are too few to yield the detailed behavior of D at $r_{ep}=0$. To show this part of coordinate space better, Figs. 11, 12, and 13 show the CFHHM and SVM values of relative local deviation in the (r_{ep},s_{ep}) coordinate system in narrow regions near the s_{ep} axis, where r_{ep} is small.

One sees that the amplitudes of the SVM values are about two orders of magnitude larger than the amplitudes of the CFHHM values at $r_{ep}\approx 0$ and s_{ep} not very small. Note that the SVM gives better relative local deviation values at $r_{ep}\approx 0$ than at $r_{ee}\approx 0$. This is because the SVM algorithm selects points predominantly in the region important for the energy, which is near the attractive coalescence point.

V. BEHAVIOR OF Ψ NEAR CUSPS

Here we show figures of $C_{ee}=(1/\Psi)(\partial\Psi/\partial r_{ee})$ and $C_{ep}=(1/\Psi)(\partial\Psi/\partial r_{ep})$, approximated by simple first-order differences on the plotting grid of points (Figs. 14–17). The CFHHM figures (Figs. 14 and 16) exhibit the correct cusp structure; since this is included analytically, only the finiteness of the grid makes the surfaces less than ideal. In the SVM, the effect of expanding Ψ on a Gaussian-type basis is much stronger than the effect of grid spacing, and the cusps are rounded instead of having strictly rectangular structure as in the CFHHM.

VI. CONCLUSION

In conclusion, we found that the amplitudes of the SVM $H\Psi/E\Psi-1$ values are consistently larger than the amplitudes of the CFHHM values in all of the coordinate space by up to five orders of magnitude, despite the fact that most SVM observables [except $\langle\delta(\mathbf{r}_k)\rangle$] converge to significantly more digits than the CFHHM observables for their respective selected bases.

The deviation of the wave function from its true value in the SVM is especially large at short distances. One should expect therefore that the expectation values of the operators getting most contributions from this region, especially δ operators, will be more precisely given by the CFHHM than by

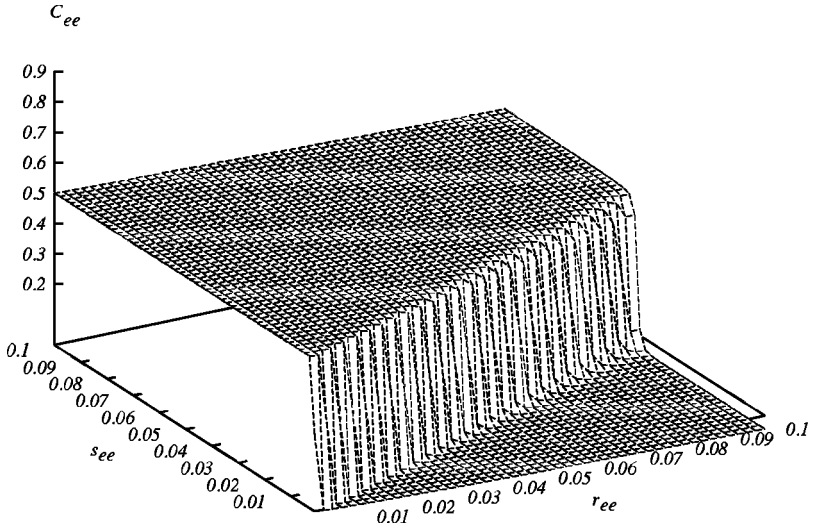

FIG. 14. $C_{ee}=(\partial\Psi/\partial r_{ee})/\Psi$ for the CFHHM, $K_{\mathrm{m}}=80$. r_{ee} and s_{ee} are in a.u.; C_{ee} is in $(\mathrm{a.u.})^{-1}$.

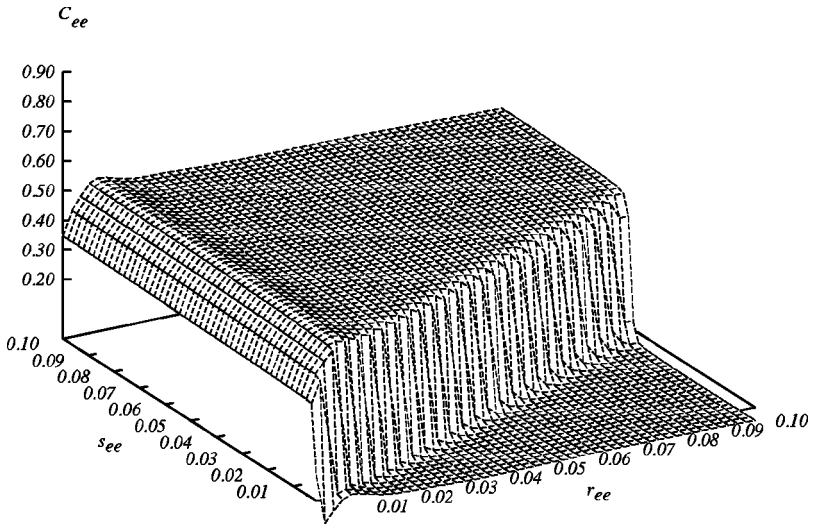

FIG. 15. As in Fig. 14, but for the SVM, $N = 800$.

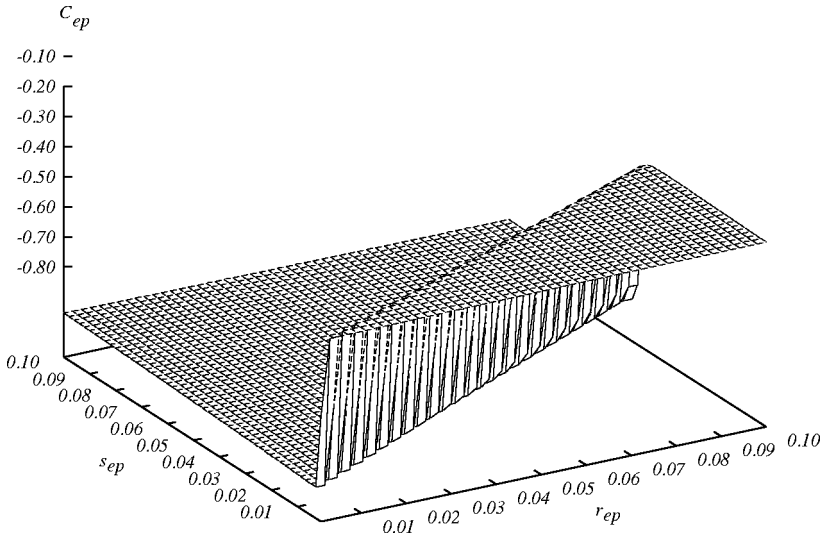

FIG. 16. $C_{ep} = (\partial\Psi/\partial r_{ep})/\Psi$ for the CFHHM, $K_{\mathrm{m}} = 80$. r_{ep} and s_{ep} are in a.u.; C_{ep} is in a.u.$^{-1}$.

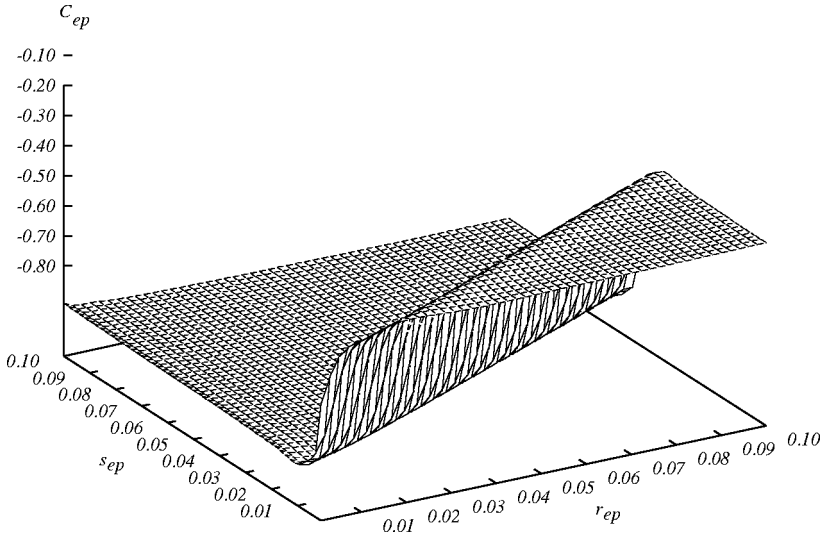

FIG. 17. As in Fig. 16, but for the SVM, $N = 800$.

the SVM. From Table I one can see that it is indeed so, and the values of $\langle \delta(\mathbf{r}_{ee}) \rangle$ and $\langle \delta(\mathbf{r}_{ep}) \rangle$ are given in the CFHHM with accuracy of two significant figures better than in the SVM. The fact that the accuracy of other short-range operators, like $\langle r_k^{-n} \rangle$, $n=1,2$, is less in the CFHHM than in the SVM has nothing to do with the accuracy of the wave function, but stems from the slower convergence of expectation values of such operators in the CFHHM due to their specific singularity at the origin (Ref. [10]). On the other hand, the better accuracy in the SVM of long-range operators like $\langle r_{ij} \rangle$ (Table I) does stem from the fact that the SVM wave function with 800 Gaussians has better asymptotics than the CFHHM with 676 hyperspherical basis functions.

Partly this is due to the fact that the f function used in the CFHHM calculation is optimized to give fast convergence of short-range operators like $\langle \delta(\mathbf{r}_k) \rangle$, and not long-range operators like $\langle r_k \rangle$ [13]. The fact that the global correction for $\langle \delta(\mathbf{r}_{ep}) \rangle$ gives errors twice as small as for the uncorrected observable in the CFHHM probably has the same origin.

The deficiency in the CFHHM asymptotics could be cured by increasing the number of basis functions or by parametrizing f with the requirement that Ψ_{CFHHM}, and not just e^f as was done for parametrization B, have proper asymptotics for a small K_{m}. However, the weaker requirement greatly simplified the determination of parameters of f [11,13], and was sufficient for the purpose of obtaining good $\langle \delta(\mathbf{r}_k) \rangle$ values.

Summing up, we have shown that direct solution of the few-body Schrödinger equation facilitating proper inclusion of cusps and analytic structure dramatically increases the quality of the wave function at all interparticle distances so far as it is characterized by the value of relative local deviation $D = H\Psi/E\Psi - 1$.

ACKNOWLEDGMENTS

The research was supported by the bilateral Cooperation Program of the Ministry of Science and Technology of Slovenia (R.K.), by The Israeli Science Foundation founded by The Israeli Academy of Sciences and Humanities (V.B.M.), and by the U.S. Department of Energy, Nuclear Physics Division, under Contract No. W-31-109-ENG-39, and OTKA Grant No. T029003 (Hungary) (K.V.). We thank Dr. R. Forrey for useful communications.

[1] J. H. Bartlett, J. J. Gibbons, and C. G. Dunn, Phys. Rev. **47**, 679 (1935).
[2] J. H. Bartlett, Phys. Rev. **98**, 1067 (1955).
[3] D. E. Freund, B. D. Huxtable, and J. D. Morgan III, Phys. Rev. A **29**, 980 (1984).
[4] M. I. Haftel and V. B. Mandelzweig, Phys. Rev. A **41**, 2339 (1990).
[5] Y. K. Ho, Phys. Rev. A **48**, 4780 (1993).
[6] K. Frankowsky and C. L. Pekeris, Phys. Rev. **146**, 46 (1966); **150**, 366(E) (1966).
[7] Y. Suzuki and K. Varga, in *Stochastic Variational Approach to Quantum Mechanical Few-Body Problems*, Vol. 54 of *Lecture Notes in Physics* edited by E. Brezin *et al.* (Springer-Verlag, Berlin, 1999).
[8] K. Varga, J. Usukura, and Y. Suzuki, Few-Body Syst., Suppl. **10**, 11 (1999).
[9] A. M. Frolov, Phys. Rev. A **57**, 2436 (1998).
[10] M. I. Haftel and V. B. Mandelzweig, Ann. Phys. (N.Y.) **189**, 29 (1989).
[11] M. Haftel, R. Krivec, and V. B. Mandelzweig, J. Comput. Phys. **123**, 149 (1996).
[12] M. Braun, W. Schweizer, and H. Herold, Phys. Rev. A **48**, 1916 (1993).
[13] R. Krivec, M. I. Haftel, and V. B. Mandelzweig, Phys. Rev. A **47**, 911 (1993).
[14] R. J. Drachman, J. Phys. B **16**, L749 (1983).